ELSEVIER

Journal of Alloys and Compounds 452 (2008) 105–109

Journal of ALLOYS AND COMPOUNDS

www.elsevier.com/locate/jallcom

Phase relations in the Ga–Mn–N system

D. Sedmidubský [a,*], J. Leitner [b], Z. Sofer [a]

[a] *Department of Inorganic Chemistry, Institute of Chemical Technology, Technická 5, 166 28 Prague, Czech Republic*
[b] *Department of Solid State Engineering, Institute of Chemical Technology, Technická 5, 166 28 Prague, Czech Republic*

Received 18 September 2006; received in revised form 21 November 2006; accepted 21 November 2006
Available online 20 January 2007

Abstract

The ternary phase diagram of the Ga–Mn–N system was constructed based on phase equilibria calculations and thermodynamic analysis of the relevant phases occurring in the studied system. Furthermore, the pesudobinary GaN–MnN_x sections for fixed nitrogen activity were calculated with a view to determine the solubility of Mn in hexagonal GaN. The used thermodynamic model relies on the assessments of the respective binary sub-systems. The only ternary phases considered are the $Ga_{1-x}Mn_xN$ solid solution, stoichiometric Mn_3GaN and the Ga–Mn–N liquid described in terms of binary Redlich–Kister parameters. *Ab initio* electronic structure calculations of cohesive energies were employed to evaluate the enthalpies of formation of some stoichiometric phases.

Keywords: Nitride materials; Dilute magnetic semiconductors; Thermodynamic modeling; Phase diagrams

1. Introduction

The gallium nitride doped by manganese and other transition metals belongs to a class of dilute magnetic semiconductors which have been recently explored as potential candidates for spintronic applications. The most promising characteristic of (Ga,Mn)N compared to more widely studied (Ga,Mn)As and (In,Mn)As is that the spin polarization persists above room temperature. However, it is still a matter of debate, whether the relatively high Curie temperature, $T_C \sim 350$ K, achieved for (Ga,Mn)N doped by 5% Mn is not due to a formation of Mn-rich ferromagnetic clusters presumably based on Mn_3GaN nucleation centers. Hence, in order to preclude these clustering effects the knowledge of the equilibrium solubility limits of Mn in GaN is of essential importance particularly for growing homogeneous thin films by MO/hydride VPE, which, unlike MBE, is considered as a close-to-equilibrium technique (with respect to the stability conditions of the deposited phase).

The aim of the present work is thus to assess the thermodynamic data of the relevant phases in the ternary system Ga–Mn–N in order to calculate the essential parts of the respective phase diagram and, in particular, to estimate the solubility of Mn in gallium nitride in its stable wurzite modification, which is in equilibrium with solid Mn_3GaN.

The starting point for the thermodynamic analysis of Ga–Mn–N system is the assessment of the relevant binary sub-systems, Ga–N, Mn–N and Ga–Mn. The thermodynamic properties of numerous non-stoichiometric phases in Mn–N system and their phase relations have been examined by Qiu and Guillermet [1], who estimated the entropies of the Mn-nitrides by analyzing their vibrational properties (force constant as a function of composition) and adjusted the enthalpies of formation to get a phase diagram according to the experimental equilibrium data. This phase diagram comprises, in addition to high temperature liquid, the solid solutions denoted as α, β, γ and δ in the Mn-rich part corresponding to the respective allotropic forms of manganese, ζ-phase ($x_N \sim 0.12$–0.3) based on hcp arrangement of Mn and three nearly stoichiometric phases ε, η, and ν with the characteristic compositions Mn_4N, Mn_3N_2, and Mn_6N_5, respectively.

The phase diagram of the metal Ga–Mn binary system has been elaborated and constructed by Lu et al. [2]. Its present form serving as a basis for this study involves several intermediate phases—the Ga-rich nearly stoichiometric compounds ω, ϕ and χ, ε (here denoted as ε′) with a narrow stability range $x_{Mn} \sim$

* Corresponding author. Tel.: +420 220 444 122.
E-mail address: sedmidub@vscht.cz (D. Sedmidubský).

0925-8388/$ – see front matter © 2007 Elsevier B.V. All rights reserved.
doi:10.1016/j.jallcom.2006.11.212

0.70–0.73, low temperature η and high temperature λ ($x_{Mn} \sim$ 0.4–0.5), γ_3 ($x_{Mn} \sim$ 0.54–0.63) and α, β, γ, γ_2 and δ in the Mn-rich part, all derived from pure Mn-phases (γ_2 from a metastable hcp-Mn).

Compared to relatively complex systems discussed above, the Ga–N binary contains only one solid phase, gallium mononitride in its stable hexagonal structure (wurtzite type), revealing only a slight nitrogen sub-stoichiometry. According to recent assessments [3,5] the high temperature liquid exhibits a miscibility gap with a critical point at $T_C \sim 4300$ K and $x_N \sim 0.3$. The stoichiometric GaN has been reported to melt incongruently at $p_{N_2} =$ 1 bar into a practically pure liquid Ga ($T_d = 1050$–1120 K), whereas a congruent melting has been predicted at 2700–2800 K and at substantially elevated pressure, $p_{N_2} \sim$ 40–90 kbar. Our recent *ab initio* calculation of $\Delta_f H_{298}$ and evaluation of entropy from normal vibration mode analysis [6] yield higher stability of GaN as against the previous works [3,5].

Last, in the ternary Ga–Mn–N system only one solid phase, Mn_3GaN with an antiperovskite structure has been known as yet, apart from the slight solubility of Mn in GaN discussed later. Since the ε-Mn_4N is the parent structure of Mn_3GaN, it is not surprising that these two form a solid solution [7]. This mutual solubility will be, however, neglected in this paper.

2. Thermodynamic model and data

Regarding the main objective of this study—the calculation of Mn-solubility in $Ga_{1-x}Mn_xN$, we aim to explore the maximum of available information from the previous assessments of the respective binary sub-systems. We thus completely adopt the data used in reference [1] to calculate the Mn–N phase diagram, despite the fact that the defect chemistry in hcp-based ζ-phase has been found more complex [8]. Unfortunately, as the form of magnetic contribution to Gibbs energy considered for Mn phases [1] is apparently different from the model implemented in FactSage [9] employed here, the magnetic term had to be neglected. This, however, brought about only a minor effect on the resulting phase diagram.

A less favorable situation exists in Ga–Mn where the available phase diagram has been constructed merely on the basis of experimental information [2] without any thermodynamic modeling. For the sake of simplicity, we consider the melt as an ideal mixture of liquid Ga and Mn and approximate the solid solutions ω, ϕ, χ, ε, η, and α by line compounds with the respective stoichiometries Ga_6Mn, Ga_3Mn, Ga_5Mn_2, $GaMn_3$, GaMn, and Mn. Although the γ_3 phase adopting the AuCu structure type should indeed represent the end-member of δ phase, it is considered as a separate stoichiometric phase, Ga_2Mn_3. The occurrence of λ and γ_2 is neglected. By contrast, the solid solubility was taken into account for β, γ and δ phases, which were modeled as mixtures of β-Mn–$GaMn_3$ and γ, δ-Mn–GaMn. In the former case, the non-ideality was described by one Redlich–Kister coefficient $L_1 = 50$–$0.045\,T$ kJ mol^{-1}, while the latter two were taken as ideal solutions.

The entropies S_{298} and heat capacities $C_p(T)$ of all line compounds and solid solution end-members were approximated by Neumann–Kopp rule with respect to the constituent elements, whereas the enthalpies of formation, $\Delta_f H_{298}$, were fitted in order to reproduce the essential features of the phase diagram [2], *i.e.* topology and incongruent melting temperatures in particular. The assessed values of $\Delta_f H_{298}$ are compiled in Table 1. Let us note that since the liquid phase is considered as ideal, the obtained $\Delta_f H_{298}$ values of solid phases are considerably higher (less exothermic) than those obtained by Miedema method.

The enthalpy of formation and entropy calculated by Sedmidubský and Leitner [6] were applied for gallium nitride in wurtzite structure, GaN(w). The $C_p(T)$ function derived from DSC and drop calorimetry data measured by Leitner et al. [10] was employed. For Ga–N liquid we preferred to use the model with two Redlich–Kister parameters as proposed by Davydov and Anderson [3] rather than the more recent one-parameter model [5], since in the former case the data for liquid nitrogen (taken from SGTE) are consistent with those used in Mn–N system [1].

The enthalpy of formation of the antiperovskite Mn_3GaN was obtained from *ab initio* total energy calculation in the same way as for GaN(w) (WIEN2k package, GGA, APW + lo basis set—for details see reference [6]). The resulting value (Table 1) was evaluated from the total energies of the pertinent phase and the corresponding elements in their standard states (for N_2a sufficiently large tetragonal unit cell was selected to simulate the gaseous state). Due to relatively complicated structure of α-Mn requiring large computational costs its total energy was calculated from that of γ-Mn and the known value of $\Delta H_{298}(\gamma - \alpha) = 4.87$ kJ mol^{-1}. As the total energies refer to $T = 0$ K, corrections were made for the $(H_{298} - H_0)$ difference. An analogous procedure was applied for MnN(w) forming the end-member of $Ga_{1-x}Mn_xN$ solution (Table 1). The detailed results of the *ab initio* calculation of cohesive energies and $\Delta_f H_{298}$ of manganese nitrides will be published elsewhere. The S_{298} and $C_p(T)$ data for MnN(w) and Mn_3GaN were taken from references [1](identified with those of γ-MnN end-member) and [11], respectively.

$Ga_{1-x}Mn_xN$ was described in terms of one-parameter regular solution model with $L_0 = 4.23$ kJ mol^{-1}, which was empirically estimated on the basis of lattice parameter mismatch between both end-members in wurtzite structure [12]. The thermodynamic behavior of Ga–Mn–N melt was modeled using the data for the liquid species as employed in the corresponding binary sub-systems as well as the binary Redlich–Kister interaction coefficients. No ternary interaction was considered in the liquid phase.

Table 1
Assessed enthalpies of formation (in kJ mol^{-1})

Phase	$\Delta_f H_{298}$	Phase	$\Delta_f H_{298}$
ω-Ga_6Mn	−65.0	ε-$GaMn_3$	−37.8
ϕ-Ga_3Mn	−43.1	β-Ga_2Mn_3	−52.0
χ-Ga_5Mn_2	−77.6	γ-GaMn	−20.8
η-GaMn	−25.8	δ-GaMn	−21.5
γ_3-Ga_2Mn_3	−58.0		
MnN(w)	−90.8	Mn_3GaN	−242.3

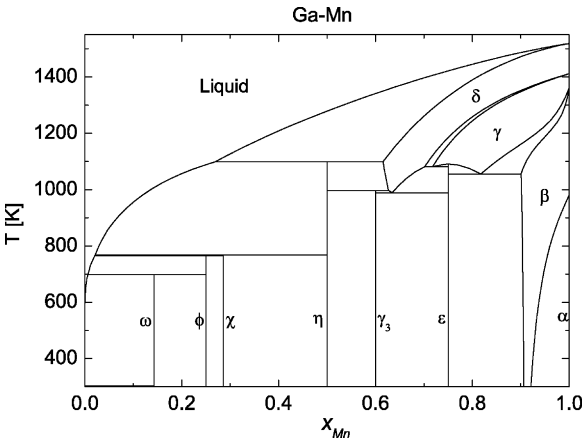

Fig. 1. Binary phase diagram of Ga–Mn system.

3. Results and discussion

All calculations of phase equilibria and phase diagram construction were carried out with the aid of FactSage 5.4.—the integrated database-Gibbs energy minimizer-phase diagram mapping system [9].

As mentioned, the thermodynamic model of Ga–Mn sub-system is very approximative and will require further revision including an indispensable experimental input. In comparison with the previously constructed diagram [2] the calculated phase diagram shown in Fig. 1 exhibits a different shape of the liquidus curve which is shifted more to Ga in the Ga-rich part (apart from the omission of λ and γ_2 phases and replacement of most solutions by stoichiometric phases). To reproduce the liquidus shape more precisely, large deviations from ideality would have to be included in the liquid phase.

The phase diagram of Mn–N system presented in Fig. 2(a) is nearly identical with the original one [1] except for the γ– ζ phase boundary which is shifted and more convex towards the Mn-rich compositions. This deflection is seemingly caused by leaving out the magnetic contributions. Moreover, we did not explicitly include the gaseous N_2 into calculation, but instead the iso-activity line was set in Fig. 2(a) representing the evolution of the overall chemical and phase composition upon heating/cooling in pure nitrogen atmosphere at normal pressure. The melting behavior of η and ν phase can be regarded only as a rough extrapolation, since in both cases invariant points refer to exceedingly high N_2 activities for which the model used here for the liquid phase is hardly applicable. The phase relations in dependence on temperature and nitrogen activity are then depicted in Fig. 2(b). Two interesting reentrant phase effects can be observed upon heating at reduced partial pressure of N_2, namely $\zeta \rightarrow \varepsilon \rightarrow \zeta$ transition at $\log(a_{N_2}) \sim -2$ and $\gamma \rightarrow \beta \rightarrow \gamma$ transition at $\log(a_{N_2}) \sim -6$.

Due to the use of revised thermodynamic data for GaN(w) reported in reference [6], its incongruent melting at normal pressure of nitrogen as well as the high pressure congruent melting and monotectic point are moved to higher temperatures—1437, 3650 and 3647 K, respectively (see Fig. 3). Using the model

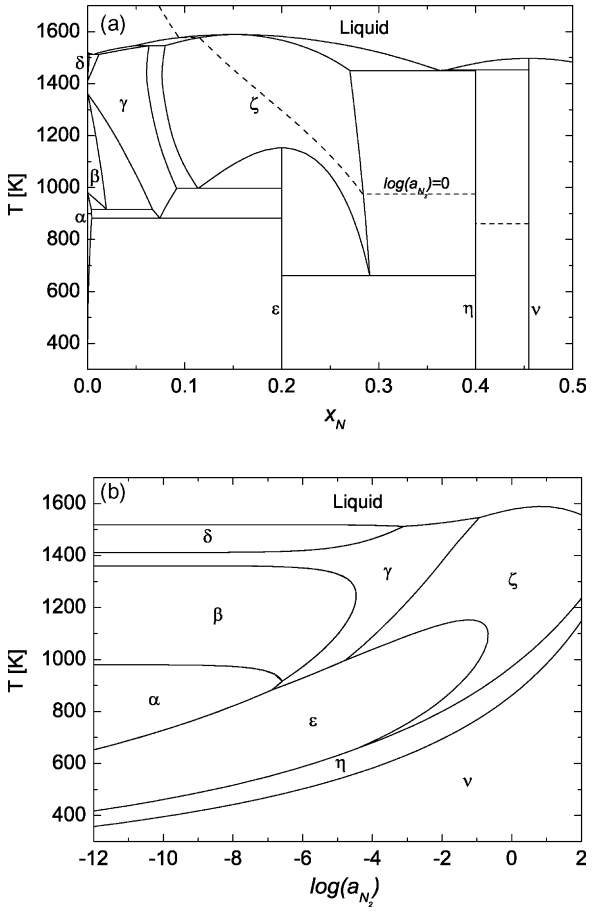

Fig. 2. Phase relations in Mn–N system. (a) x_N–T phase diagram, (- - -) iso-activity line for $a_{N_2} = 1$. (b) a_{N_2}–T phase diagram.

for real N_2gas [4] a value of $p_{N_2} = 5.9$ GPa comes out for the nitrogen pressure corresponding to congruent melting point, T_m. This is consistent with $p_{N_2} = 4.9$ GPa obtained by Davydov et al. [4] for $T_m = 2792$. It must be noted, however, that our p_{N_2} represents only a rough estimate, since the model equation was extrapolated by ~900 K above the guaranteed temperature range.

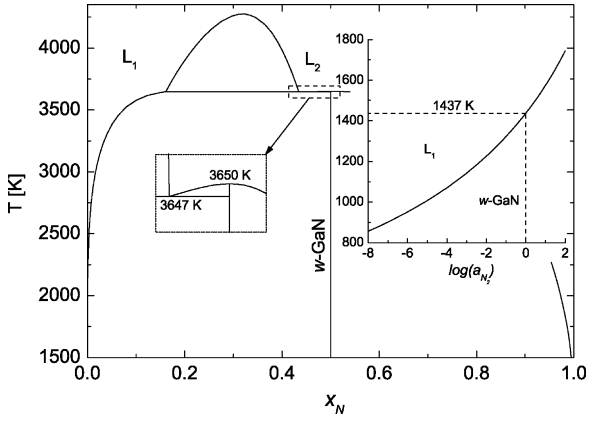

Fig. 3. Binary phase diagram of Ga–N system. Right inset: phase boundary line of GaN(w) incongruent melting as a function of T and a_{N_2}, left inset: a blow-up of GaN(w) congruent melting and monotectic point.

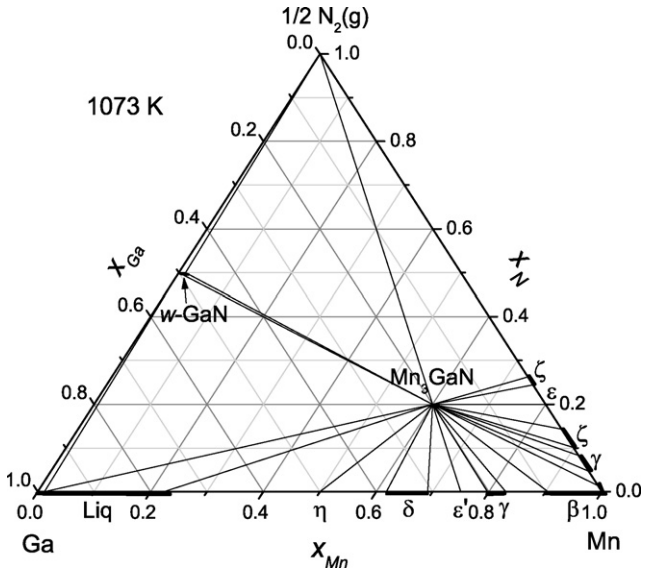

Fig. 4. Ternary phase diagram of Ga–Mn–N system calculated for $T = 1073$ K.

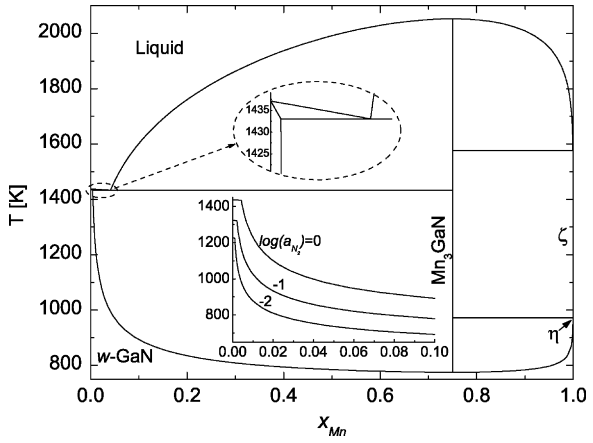

Fig. 5. Iso-activity section of Ga–Mn–N phase diagram for $a_{N_2} = 1$. The Mn content, x_{Mn}, refers to a total mole amount of Mn + Ga. Inset: solubility of Mn in $Ga_{1-x}Mn_xN$ for different values of a_{N_2}.

The discrepancy between the decomposition temperature $T_d = 1437$ K ($a_{N_2} = 1$) obtained from our data and that reported by Unland et al. [5], including the compiled experimental values (scattered in the interval $T_d = 975$–1330 K), has been already discussed in reference [6]. It has been argued that the simple model of GaN(w) decomposition into pure liquid Ga and gaseous N_2seems to be inadequate and a revision of the model for Ga–N liquid and/or a more realistic model for GaN(w), involving, *e.g.* formation of N-vacancies, would be necessary to bring the calculated equilibrium in accordance with experiment. Nevertheless, the phase diagram of Ga–Mn–N system presented in this work and particularly the $Ga_{1-x}Mn_xN$ homogeneity range are believed to be little affected by this inconsistency.

First glance at the ternary Ga–Mn–N isothermal phase diagram (Fig. 4) calculated for $T = 1073$ K, which is the supposed optimal temperature of $Ga_{1-x}Mn_xN$ deposition, reveals an unusual stability of Mn_3GaN phase being in equilibrium with almost all phases occurring in the system. Since this applies also for the Mn_3GaN–Mn_4N tie-line, the appearance of the isothermal section would not be likely altered if the solubility between these two phases was taken into account.

As the upper corner of the phase diagram is represented by gaseous N_2 in its standard state ($a_{N_2} = 1 \sim p_{N_2}/p^\circ$), $Ga_{1-x}Mn_xN$(w) solid solution, Mn_3GaN and ζ-phase are all in equilibrium with nitrogen gas at these conditions. By contrast, the equilibria with liquid phase and the solid solutions in the Mn-rich part all correspond to significantly reduced nitrogen activity.

The solubility of 2.4 at% of Mn in the wurtzite $Ga_{1-x}Mn_xN$ phase is predicted for the selected conditions. Within this homogeneity range, $Ga_{1-x}Mn_xN$ is in equilibrium with Mn_3GaN and N_2(g), only an unrecognizably narrow compositional range contiguous to the GaN end-member is also in equilibrium with the Ga-rich melt. It is apparent from the iso-activity section constructed for $a_{N_2} = 1$ (Fig. 5) that the limited solubility of Mn in GaN(w) is not of intrinsic type due to a miscibility gap caused by large positive deviation from the ideality (repulsive Mn–Ga interaction), but it rather results from the competition with the stability of Mn_3GaN phase. The high stability of Mn_3GaN also eliminates all other phases from the game and reduces the problem of finding the solubility of Mn to solving a simple equilibrium GaN(w) + 3MnN(w) ↔ Mn_3GaN + $3/2N_2$.

The obtained result for the assumed deposition conditions ($T \sim$1000–1300 K) seems to be quite reasonable, but the complete solubility observed below 775 K is most likely unrealistic. However, one would have to go beyond the simple regular solution model to get the limited solubility for lower temperatures without affecting the high temperature part. Moreover, the calculated iso-activity section (Fig. 5) is not consistent with the already published Mn–N phase diagram [1] where the MnN(w) phase is completely missing. The only stable representative of the MnN family is the ν-phase here approximated by Mn_6N_5, which is in fact a nitrogen deficient, tetragonally distorted MnN_{1-x} in rock-salt structure. To get an agreement, either the stability of MnN(w) (*ab initio* value of $\Delta_f H_{298}$) would have to be decreased or a complete re-assessment of Mn–N system would be necessary. In the present phase diagram, MnN(w) end-member transforms directly to η (Mn_6N_4) being stable only in a very narrow temperature range (depicted as a horizontal line in Fig. 5), which further transforms to ζ-phase.

Shown in the inset of Fig. 5 is further the effect of reduced activity of nitrogen on the gradual narrowing of $Ga_{1-x}Mn_xN$ homogeneity range. This might be of importance particularly for the deposition of thin films by MOVPE and yet more by MBE being operated at low pressures. It should be however noted that the current model applies for a bulk material whose thermodynamic properties might be markedly modified when deposited as a thin layer on a substrate. The experimental results obtained on various Mn-doped semiconductor systems suggest that Mn solubility is indeed enhanced when the material is prepared in the form of thin films.

4. Conclusions

This study represents the first attempt to assess the thermodynamic properties of phases in ternary Ga–Mn–N system with a focus to predict the homogeneity range of wurtzite type $Ga_{1-x}Mn_xN$ solid solution. The predicted solubility of a few atomic percent of Mn in the range of the assumed optimal synthesis conditions seems to be satisfactory and reasonable, however, a controversy still persists in the low temperature range where a complete miscibility GaN(w)–MnN(w) is obtained. A further refinement of the thermodynamic model and an involvement of new experimental data are thus highly desirable.

Acknowledgements

Supported by the Czech Science Foundation, grant no. 104/06/0642, and the Ministry of Education of Czech Republic, project no. MSM6046137302.

References

[1] C. Qiu, A.F. Guillermet, Z. Metalkd. 84 (1993) 11.
[2] X.S. Lu, J.K. Liang, M.G. Zhu, Acta Phys. Sinica 29 (1980) 469.
[3] A.V. Davydov, T.J. Anderson, Electrochem. Soc. Proc. 98-18 (1999) 38.
[4] A.V. Davydov, W.J. Boettinger, U.R. Kattner, T.J. Anderson, Phys. Status Solidi (a) 188 (2001) 407.
[5] J. Unland, B. Onderka, A. Davydov, R. Schmid-Fetzer, J. Cryst. Growth 256 (2003) 33.
[6] D. Sedmidubský, J. Leitner, J. Cryst. Growth 286 (1) (2006) 66.
[7] M. Barberon, R. Madar, E. Fruchart, G. Lorthioir, R. Fruchart, Mater. Res. Bull. 5 (1970) 903.
[8] A. Leineweber, H. Jacobs, W. Kocklemann, J. Alloys Compd. 368 (2004) 229.
[9] FactSageTM, Version 5.4.1, 2005 Thermfact Ltd. & GTT-Technologies mbH, www.factsage.com.
[10] J. Leitner, A. Strejc, D. Sedmidubský, K. Ružička, Thermochim. Acta 401 (2) (2003) 169.
[11] J. García, J. Bartolomé, D. González, R. Navarro, D. Fruchart, J. Chem. Thermodyn. 15 (1983) 1041.
[12] J. Leitner, J. Phys. Chem. Solids 58 (1997) 1329.